

STABILIZATION OF SUPERIONIC α -AgI AT ROOM TEMPERATURE IN POLYMER MATRICES BY BALL MILLING

H. Z. LIU^a, X. ZHONG^a, H. Y. XIAO^{a*}, H. JIANG^b, H.F. ZHAO^b, X. P. LIU^c

^aState Key Laboratory of Silicate Materials for Architectures, Wuhan University of Technology, Wuhan 430070, China.

^bState Key Laboratory of Special Glass, Haikou 571924, Hainan, China

^cJiangsu Ruihe Abrasives co., ltd., Yancheng 224051, Jiangsu, China

To stabilize high ionic conductive α -phase of AgI to ambient temperature, (1-x)AgI •xPVP (poly-N-vinyl-2-pyrrolidone) composites were synthesized by high energy planetary ball milling techniques. Phase transition temperature (T_c) of α to β/γ for AgI shifts considerably to lower temperature with the increase of PVP content, simultaneously leading to progressively enlarged thermal hysteresis. Specifically, when x approaches to 0.8, the α -phase survives down to 21 °C, which, to the best of our knowledge, is the lowest temperature for the reported AgI family material.

(Received June 19, 2017; Accepted August 23, 2017)

Keywords: α -AgI, Phase transition, Room temperature, Ball milling

1. Introduction

Recently, Super-Ionic conductor materials are widely studied for their promising application potential in batteries and sensors^[1-2], which include oxide series^[3-5], chalcogenide series^[6-12] and halogen series^[13-14] of conductor materials. High temperature α -phase of silver iodide (AgI) shows very high ionic conductivity greater than 1 S.cm⁻¹, however, it transforms to poorly conducting β -/ γ - phase when the temperature is below 147 °C. Many works have been conducted to stabilize high ionic conductive α -phase to ambient temperature.

Masahiro tatsumisago et al^[15] reported that they had stabilized α -AgI at room temperature in a AgI–Ag₂O–B₂O₃ glass matrix through rapid melt-quenching techniques. However, such stabilization is irreversible and after sequential thermal cycling, the high ionic conductive α -phase disappears at 110 °C in cooling runs. Another feasible route to stabilize the superionic phase to lower temperature is to control the size and shape of nanoscaled AgI. When the size of materials is restricted to nm-order, the increasing ratio of surface atom will increase the interfacial energy, resulting in the decrease of lattice fusion/melting and order-disorder phase transition temperature^[16-17].

Liang et al. embedded the 6 nm-size around AgI nanowires in an anodic-aluminum-oxide by template-assisted method, the high conductive phase remained at the temperature of 80 °C^[18]. M. Hanaya inserted AgI in the porous silica with different pore from 50 to 10 nm by applying a salt-bridge precipitation technique. The α to β/γ phase transition temperature was observed to become lower remarkably with the decrease of AgI crystal size, the lowest temperature was 98 °C when the size of AgI crystal reached to 10 nm^[19]. Rie Makiura employed PVP as a stabilizer to coat 10-11 nm AgI particle, the high-temperature phase can be kept at 40 °C^[20]. Thereby, we assume that the key factor influencing the lowering of phase change temperature is the chemical environment around the AgI crystal.

*Corresponding authors: 200542@whut.edu.cn

In this work, we employed a very convenient method to stabilize α -AgI at room temperature, that is to coat AgI crystal with PVP by high energy ball-milling technique^[20] rather than change the size of AgI crystal. Through the systematic characterization of calorimetric and mass response of the $(1-x)\text{AgI}\cdot x\text{PVP}$ composite together with their XRD patterns, the mechanism of β/γ to α and α to β/γ phase transition process was investigated in detail.

2. Experimental

2.1. Materials

The $(1-x)\text{AgI}\cdot x\text{PVP}$ were obtained by a high energy planetary ball milling machine (Fritsch Pulverisette 7). AgI (Aladdin) and Polyvinylpyrrolidone (Aladdin, K88-96; average MW = 1300000) were weighed with different molar ratio x ($x=0.2,0.5,0.8$) of $(1-x)\text{AgI}\cdot x\text{PVP}$. Then transferred into a 20 ml ZrO_2 pot. Weight ratio of ball (3 mm ZrO_2 balls in diameter) and the composite is 1:15.

2.2. Characterization

Crystal phase analysis was conducted by X-ray diffraction method (RU-200B, Rigaku, Tokyo, Japan) with $\text{Cu K}\alpha$ radiation at room temperature. DSC measurements were carried out with a PerkinElmer DSC8000 instrument in the range 0-180 °C with a typical sweeping rate of 10 K/min in N_2 . TGA measurements were carried out with a NETZSCH STA 449 F1 DSC in the range 40-180 °C with a typical sweeping rate of 10 K/min in Ar.

3. Results

To figure out whether the surface defects on the crystal AgI caused by high-energy ball milling process influence the phase transition temperature, we conducted one group DSC comparison experiment of raw AgI sample and as milled AgI sample. As shown in Fig. 1, we can find that in the heating process, two samples exhibited endothermic effect at around 150 °C, this thermal anomaly is reasonably considered due to the phase transition from β/γ to α phase of crystal AgI. The peak temperature is defined as the phase transition temperature. $T_{c\uparrow}$ of as-milled AgI sample shifts lightly to lower temperature compared to the raw AgI crystals, which can be considered due to the size effects^[21]. In the cooling process, $T_{c\downarrow}$ shifts from 143 °C to 133 °C, we will discuss it in the following section.

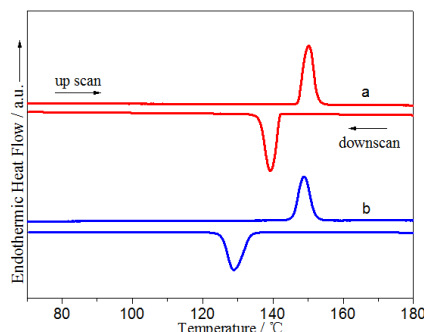


Fig.1. DSC results of AgI crystal (a) and the as-milled AgI powder prepared at 800 rpm for 2hrs (b). The upscan and downscan rates are 10K/min.

In order to further modify the phase transition process of AgI, PVP was added to coat on the surface by milling $(1-x)\text{AgI}\cdot x\text{PVP}$ at 800 rpm for 2 hrs. As shown in Fig. 2(a, b, c), in the first

heating run, there appeared a broad endothermic peak at low temperature range; however, in the second heating run, the broad endothermic peak at low temperature range disappeared. We attribute it to the volatilization of smaller molecular PVP caused by the ball-milling process, which can be further verified by the data shown in Fig.2(d). In the first heating run, weight loss, which increases following the further addition of PVP molecule, can be clearly seen. In the second heating run, the mass almost remain a constant. Furthermore, the α to β/γ phase transition peak slightly shifts to lower temperature compared with the one in the first heating run. During the two cycles of cooling runs, no clear difference of phase change temperature ($T_{c\downarrow}$) occurs except for the 0.8AgI-0.2PVP sample. $T_{c\downarrow}$ shifts to about 71 °C, 30 °C and further to 21 °C following the addition of PVP from 0.2, 0.5, to 0.8. As far as we know, 21 °C is the lowest α to β/γ phase transition temperature for any AgI family material.

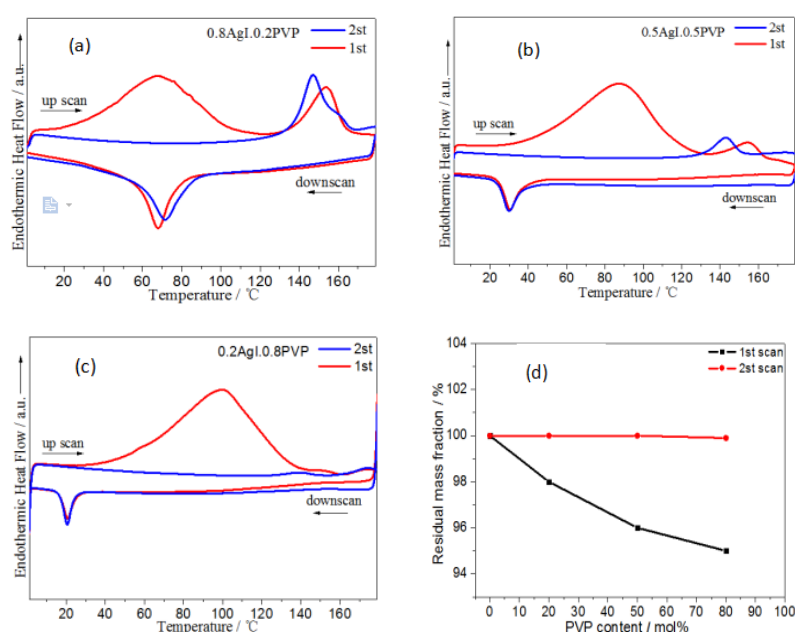


Fig. 2. Upscan and downscan DSC curves of sequential two cycles for the as-milled 0.8AgI • 0.2PVP(a), 0.5AgI • 0.5PVP(b) and 0.2AgI • 0.8PVP(c) samples prepared at 800 rpm for 2 hrs.(d) Residual mass plot of sequential two cycles for the three samples. The upscan and downscan rates are 10 K/min.

To explore whether there exist some chemical reactions between PVP and AgI crystal during the high energy ball mill process, X-ray diffraction method was carried out at room temperature. As shown in Fig. 3, it appears apparent β/γ phase feature for all three samples.

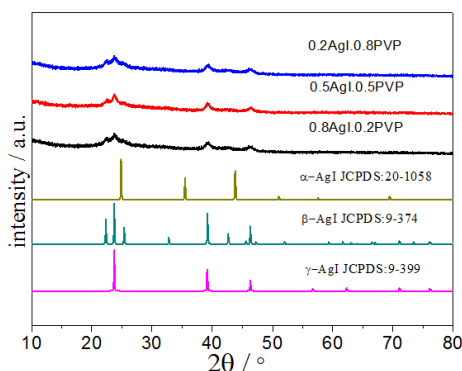


Fig. 3 XRD patterns of the as-milled $(1-x)\text{AgI} \cdot x\text{PVP}$ samples prepared at 800 rpm for 2 hrs, together with $\alpha\text{-AgI}$ (JCPDS: 20-1058), $\beta\text{-AgI}$ (JCPDS: 9-374) and $\gamma\text{-AgI}$ (JCPDS: 9-399).

4. Discussion

Compared to the raw AgI crystal, $T_{c\uparrow}$ of as-milled AgI sample shifts slightly to lower temperature as shown in Fig. 1, which can be considered to be due to the size effect. During the cooling process, $T_{c\downarrow}$ shifts from 143 °C to 133 °C, which is well above the room temperature. So we can conclude that the size effects and surface defects caused by the high-energy ball milling process have not enough influence to the $T_{c\downarrow}$ without adding any other agent.

When PVP was employed to coat AgI particle, three groups of $(1-x)\text{AgI} \cdot x\text{PVP}$ mixed powder was synthesized by milling at 800 rpm for 2 hrs. According to the DSC curves of Fig. 2(a, b, c), we can find that at the first thermal cycle for three samples, during the heating process, there appears a broad endothermic peak in low temperature range; however, in the second heating runs, the broad endothermic peak at lower temperature disappeared, which maybe be attributed to the volatilization of smaller molecular PVP caused by the ball-milling process as shown in Fig.2(d). There exist a weight-loss for all three samples in the first runs; but remain constant during the second and further runs. After the smaller molecular PVP evaporates, some nano- or micro-pores will appears in the samples, which can lower the thermal conduction, resulting in a slight increase of the peak temperatures compared with the raw AgI crystal. As shown in Fig. 4(b), for all samples in first up-scan, $T_{c\uparrow}$ is above 149 °C. When the content of PVP increases, $T_{c\uparrow}$ shifts to lower temperature, which maybe originated from the high thermal conductivity of PVP molecules. Contrast to this, the phenomenon, that $T_{c\uparrow}$ shifts to higher temperature, occurs when AgI particles was covered by the coatings with lower thermal conductivity, such as Al_2O_3 , SiO_2 , P_2S_5 etc^[19,22-24]. However, when it comes to the second heating cycle, the gradual drop for the phase change temperature occurs, which possibly can be ascribed to the synergetic effects of enhancement of thermal conductivity due to the rearrangement of larger PVP molecules leading to the shrinkage of pores in the samples as well as the effect of reduced size for AgI.

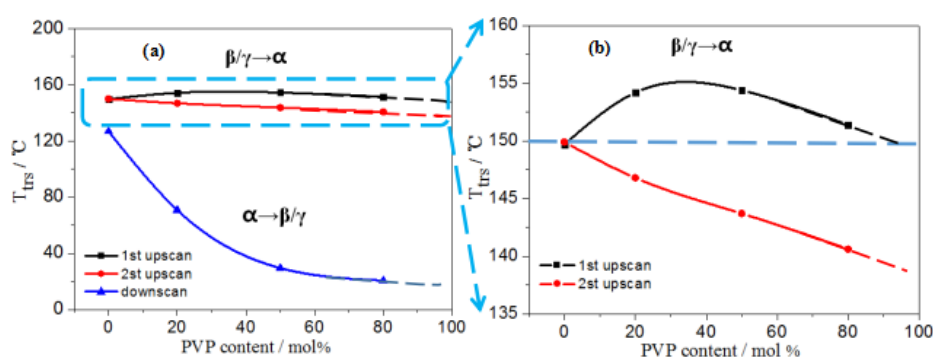


Fig. 4. PVP content dependence of the phase transition temperature, T_{trs} . (a): the black square and red circle represent the results for β/γ to α phase transition observed in first and second heating runs, and blue triangle for α to β/γ phase transition in cooling runs. (b): the partial enlarged detail of plot (a).

During cooling runs, all the samples appear exothermic peak which can be due to the phase transition of AgI crystal from β/γ to α phase. $T_{c\downarrow}$ was observed to become lower remarkably with the increase of PVP content, when the amount of PVP reach 80 %, $T_{c\downarrow}$ is suppressed down to 21 °C. It could be contrasted with the small change of the $T_{c\uparrow}$ during heating runs with the change of the PVP content. The α to β/γ phase transition temperature almost identical at one PVP content for the sequential two thermal cycles. It indicates that the low-temperature stabilization of α -AgI is reversible. Rie Makiura^[20] attributed the suppression of the phase transition not only to the increase of the surface energy, but also to the presence of defects and the accompanying charge imbalance induced by PVP when the diameter of AgI particles reach around 10 nm. What we emphasize is that the size of our as-milled AgI particle is above 100 nm according to previous related work, also occur a huge hysteresis phenomenon on cooling. One possible reason is that in the α -AgI, highly mobile Ag^+ ions exist at the interface between the coating PVP and the AgI particle, could diffuse into the polymer, whereas the I ions stay on the surface of the AgI particle. It results in the generation of an assignable number of lattice defects, causing a charge imbalance. The more the PVP content, the more obvious effect of the charge imbalance. It means that the pronounced charge imbalance effect play a major role on the suppression of the phase transition from α to β/γ phase, this is consistent with Rie Makiura's work.

The phase transition from α to β/γ phase could be recognized as the process of nucleation and growth^[25-27]. The energetic models for the α to β/γ phase transformation of AgI in the different content of PVP. As shown in Fig. 5 a, b and c, are based on the comparison of the transformation behaviors observed in cooling curves of DSC. ΔG_{total} denotes the total free energy change on formation of a spherical β/γ -AgI nucleus in an α -AgI particle. ΔG_{total} can be showed as the following equation^[23]

$$\Delta G_{total} = G_{\beta/\gamma} - G_{\alpha} = 4/3\pi r^3 \Delta G_c + 4\pi r^2 \Delta \gamma + 4/3\pi r^3 \Delta \epsilon \quad (1)$$

Respectively, G_{α} , and $G_{\beta/\gamma}$, are the free energies of α and β/γ phase, r is the nucleus radius, ΔG_c is the volume free energy change per unit volume, $\Delta \gamma$ is the surface free energy change per unit area, $\Delta \epsilon$ is the strain energy change per unit volume. Besides, ΔG^* is the nucleation barrier, controlling the α to β/γ transformation rate.

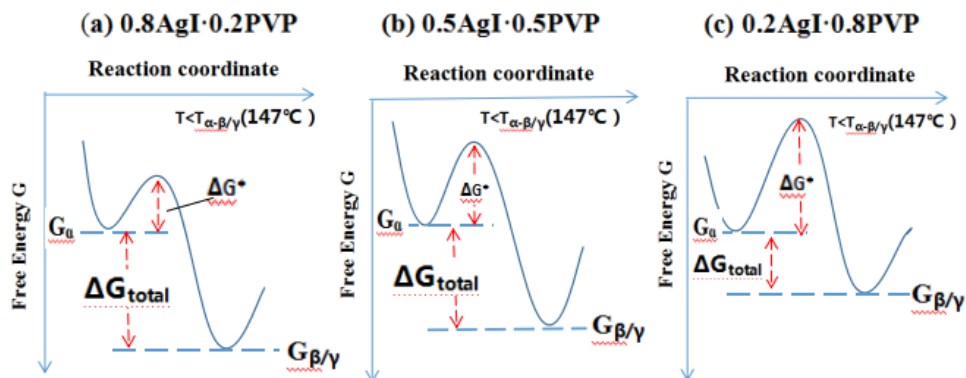


Fig.5. The reaction coordinate diagrams for the transformation of α -AgI crystal to the β/γ -phase for three samples: 0.8AgI·0.2PVP (a), 0.5AgI·0.5PVP (b) and 0.2AgI·0.8PVP (c).

Therefore, there should exist a relationship as $\Delta G^*(a) < \Delta G^*(b) < \Delta G^*(c)$. Thus, when cooling, the super-cooling of phase transition temperature from α -AgI to β/γ -AgI should be ascribed to the retardation of the nucleation of the ordered phase of β/γ -AgI with the increase of the PVP content.

5. Conclusions

In this work, the high energy planetary ball milling method was applied to prepare the (1-x)AgI·xPVP composites. Following the addition of PVP, the α to β/γ phase transition temperature for AgI shifts to lower temperature. When the concentrate of PVP arrives at 0.8, the phase transition temperature from α to β/γ when cooling occurs reversibly at about 21 °C. This work gives us a clue to obtain the high temperature phase stabilized down to Room temperature, which may be applied to other phase change materials, such as VO₂.

Acknowledgement:

This work was financially supported by NSFC (No.51372180), the Key Technology Innovation Project of Hubei Province (2016AAA029) and Innovation and entrepreneurship leading talent for Yancheng city and Jiangsu province. H. Z. Liu and X. Zhong contributed equally to this work and should be considered co-first authors.

References

- [1] A. S. Aricò, P. Bruce, B. Scrosati, Nature Materials **4**, 366 (2005).
- [2] Y. G. Guo, J. S. Hu, L. J. Wan, Advanced Materials **20**, 2878 (2008).
- [3] H. P. Chen, H. Z. Tao, Q. D. Wu, X. J. Zhao, Journal of the American Ceramic Society **96**, 801 (2013).
- [4] S. Liu, Y. Kong, H. Tao, and Y. Sang, Journal of the European Ceramic Society **37**, 715 (2017)
- [5] Z. T. Shan, C. J. Li, H. Z. Tao, Journal of the American Ceramic Society **00**, 1 (2017).
- [6] A. Qiao, H. Z. Tao, Y. Z. Yue, Journal of the American Ceramic Society **100**, 968 (2017).

- [7] X. Han, H. Tao, L. Gong, X. Wang, X. Zhao, Y. Yue, *Journal of Non-Crystalline Solids* **391**, 117 (2014).
- [8] H. Tao, X. Zhao, Q. Liu, *Journal of Non-Crystalline Solids* **377**, 146 (2013).
- [9] H. Z. Tao, Z. Y. Yang, P. Lucas, *Optics Express* **17**, 18165 (2009).
- [10] C. Lin, H. Tao, X. Zheng, R. Pan, H. Zang, X. Zhao, *Optics Letters* **34**, 437 (2009).
- [11] H. Tao, C. Lin, S. Gu, C. Jing, X. Zhao, *Applied Physics Letters* **91**, 475 (2007).
- [12] A. Qiao, H. Yang, H. Y. Xiao, J. Xiao, X. P. Liu, Z. R. Ge, R. H. Chen, *Chalcogenide Letters* p.195 (2016).
- [13] G. Dong, H. Tao, X. Xiao, C. Lin, Y. Gong, X. Zhao, S. Chu, S. Wang, and Q. Gong, *Optics Express* **15**, 2398 (2007).
- [14] S. Yan, H. Xiao, X. Liu, *Chalcogenide Letters* **13**, 483 (2016).
- [15] M. Tatsumisago, Y. Shinkuma, T. Minami, *Nature* **354**, 217 (1991)
- [16] P. Sheng, R. W. Cohen, J. R. Schrieffer, *Journal of Physics C Solid State Physics* **14**, L565 (1981).
- [17] H. Z. Tao, T. D. Bennett, Y. Z. Yue, *Advanced Materials* **29**, 1601705-1 (2017).
- [18] C. Liang, K. Terabe, T. Hasegawa, M. Aono, I. N, *Journal of applied physics* **102**, 124308 (2007).
- [19] M. Hanaya, I. Osawa, K. Watanabe, *Journal of Thermal Analysis and Calorimetry* **76**, 529 (2004).
- [20] R. Makiura, T. Yonemura, T. Yamada, M. Yamauchi, R. Ikeda, H. Kitagawa, K. Kato, M. Takata, *Nature materials* **8**, 476 (2009).
- [21] I. V. Chernyshova, M. F. Hochella Jr, A. S. Madden, *Physical Chemistry Chemical Physics* **9**, 1736 (2007).
- [22] C. Liang, K. Terabe, T. Hasegawa, *Journal of Applied Physics* **102** 415 (2007)
- [23] H. Yang, X. P. Liu, Z. R. Ge, R. H. Chen, H. Tao, *Digest Journal of Nanomaterials and Biostructures* **12**, 303(2017).
- [24] W. D. Kingery, H. K. Bowen, D.R. Uhlmann, *Introduction to Ceramics* p, 328 (1976).
- [25] M. J. Zhang, Z. Y. Yang, L. Li, Y. W. Wang, J. H. Qiu, A. P Yang, H. Z. Tao, D. Y. Tang, *Journal of Non-Crystalline Solids* **452**, 114 (2016).
- [26] M. J. Zhang, Z. Y. Yang, H. Zhao, A. P. Yang, L. Li, H. Z. Tao, *Journal of Alloys and Compounds* **722**, 166 (2017).
- [27] T. Saito, M. Tatsumisago, N. Torata, T. Minami, *Solid State Ionics* **79** 279 (1995).